The p.Arg63Trp polymorphism controls Vav1 functions and Foxp3 regulatory T cell development

Céline Colacios,[1,2,3] Audrey Casemayou,[1,2,3] Anne S. Dejean,[1,2,3] Frédérique Gaits-Iacovoni,[4] Christophe Pedros,[1,2,3] Isabelle Bernard,[1,2,3] Dominique Lagrange,[1,2,3] Marcel Deckert,[5] Lucille Lamouroux,[1,2,3] Maja Jagodic,[6] Tomas Olsson,[6] Roland S. Liblau,[1,2,3] Gilbert J. Fournié,[1,2,3] and Abdelhadi Saoudi[1,2,3]

[1]Institut National de la Santé et de la Recherche Médicale Unité 1043, [2]Centre National de la Recherche Scientifique Unité 5282, and [3]Université de Toulouse, Université Paul Sabatier, Centre de Physiopathologie de Toulouse Purpan, Toulouse F-31300, France
[4]Institut National de la Santé et de la Recherche Médicale Unité Mixte de Recherche 1048, Institut des Maladies Métaboliques et Cardiovasculaires Toulouse F-31300, France
[5]Institut National de la Santé et de la Recherche Médicale Unité 1038, Université de Nice Sophia-Antipolis, Nice 06202, France
[6]Neuroimmunology Unit, Department of Clinical Neuroscience, Karolinska Institutet, S-17176 Stockholm, Sweden

CD4+ regulatory T cells (T_{reg} cells) expressing the transcription factor Foxp3 play a pivotal role in maintaining peripheral tolerance by inhibiting the expansion and function of pathogenic conventional T cells (T_{conv} cells). In this study, we show that a locus on rat chromosome 9 controls the size of the natural T_{reg} cell compartment. Fine mapping of this locus with interval-specific congenic lines and association experiments using single nucleotide polymorphisms (SNPs) identified a nonsynonymous SNP in the *Vav1* gene that leads to the substitution of an arginine by a tryptophan (p.Arg63Trp). This p.Arg63Trp polymorphism is associated with increased proportion and absolute numbers of T_{reg} cells in the thymus and peripheral lymphoid organs, without impacting the size of the T_{conv} cell compartment. This polymorphism is also responsible for Vav1 constitutive activation, revealed by its tyrosine 174 hyperphosphorylation and increased guanine nucleotide exchange factor activity. Moreover, it induces a marked reduction in Vav1 cellular contents and a reduction of Ca^{2+} flux after TCR engagement. Together, our data reveal a key role for Vav1-dependent T cell antigen receptor signaling in natural T_{reg} cell development.

CORRESPONDENCE
Abdelhadi Saoudi:
abdelhadi.saoudi@inserm.fr

Abbreviations used: ACI, August Copenhagen Irish; BB, Biobreeding; BN, Brown Norway; CH, calponin homology; DA, Dark Agouti; DP, double positive; GEF, guanine exchange factor; LEW, Lewis; mRNA, messenger RNA; PVG, Piebald Virol Glaxo; SNP, single nucleotide polymorphism; SP, single positive.

Naturally derived regulatory T cells (T_{reg} cells) are generated in the thymus and play a pivotal role in preventing pathological immune responses including autoimmunity, inflammation, and allergy (Sakaguchi et al., 2008). Foxp3, a member of the forkhead transcription factors, has been identified as the master regulator for the development and function of T_{reg} cells (Zheng and Rudensky, 2007). Deficiencies in Foxp3 cause a lethal lymphoproliferative disorder in scurfy mice and are associated with immunodysregulation, polyendocrinopathy, enteropathy, and X-linked syndrome in humans. A study using Foxp3-GFP reporter mice revealed that Foxp3 expression is associated with suppressor activity irrespective of CD25 expression (Fontenot et al., 2005). Finally, the maintenance of Foxp3 expression in mature T_{reg} cells is needed to sustain the transcriptional and functional program established during T_{reg} cell development. These findings demonstrate that Foxp3 acts as a T_{reg} cell lineage specification factor, programming the development and the suppressive activity of T_{reg} cells.

Thymic differentiation of T_{reg} cells is instructed by the intensity of signaling via the TCR and is regulated by co-stimulatory receptors

C. Colacios and A. Casemayou contributed equally to this paper.
G.J. Fournié and A. Saoudi contributed equally to this paper.

The Rockefeller University Press $30.00
J. Exp. Med. Vol. 208 No. 11 2183-2191
www.jem.org/cgi/doi/10.1084/jem.20102191

such as CD28 and cytokines, including IL-2 (Josefowicz and Rudensky, 2009). TCR signaling controls T_{reg} cell and conventional T cell (T_{conv} cell) development differently. T_{reg} cell development is favored under conditions of TCR signaling with high strength that promotes negative selection of T_{conv} cell (Jordan et al., 2001; Hsieh et al., 2004; Carter et al., 2005). In addition, deficiency of several pleiotropic signaling molecules, including TAK1, Bcl10, CARMA1, PKC-θ, IKK-β, c-Rel, LAT, and Foxo1/Foxo3a proteins, severely impairs T_{reg} cell development, whereas it only marginally affects T_{conv} cell development (Koonpaew et al., 2006; Wan et al., 2006; Gupta et al., 2008; Medoff et al., 2009; Ouyang et al., 2010). However, the signaling pathways precisely involved in T_{reg} cell development remain poorly characterized.

Vav1 is a key signal transducer downstream of the TCR and is mandatory for the development and activation of T cells (Turner and Billadeau, 2002; Tybulewicz, 2005). In the present study, we demonstrate a major role for Vav1 protein in natural T_{reg} cell development. The analysis of the genetic factors responsible for the difference in the size of the T_{reg} cell compartment between two rat strains led to the identification of a nonsynonymous polymorphism in the first exon of *Vav1*, responsible for the substitution of an arginine by a tryptophan at position 63 (p.Arg63Trp or R63W). Associated with this substitution, we observed an increased proportion and absolute numbers of T_{reg} cells in peripheral lymphoid organs, which most likely result from an increased output of T_{reg} cells from the thymus. The Vav1-W63 variant is constitutively active, and its cellular protein levels are markedly reduced. This is associated with a decrease in Ca^{2+} mobilization under TCR activation. Thus, our study highlights the importance of Vav1 in T_{reg} cell development and the role that Vav1 signaling alterations could play in susceptibility to immune diseases.

RESULTS AND DISCUSSION

Brown Norway (BN) rats have higher proportions and absolute numbers of CD4$^+$Foxp3$^+$ T_{reg} cells than Lewis (LEW) rats

We investigated CD4$^+$Foxp3$^+$ T_{reg} cell development in LEW and BN rats, two strains which differ strikingly in their susceptibility to immune diseases (Fournié et al., 2001). Flow cytometry analysis of CD4$^+$Foxp3$^+$ T cells in PBMCs, LNs, and spleen revealed that the proportion (Fig. 1 A) and absolute numbers (Fig. 1 B) of Foxp3$^+$ cells among CD4$^+$ T cells were significantly higher in BN than in LEW rats. Similar results were observed in double-positive (DP) CD4$^+$CD8$^+$ and single-positive (SP) CD4$^+$CD8$^-$ thymocytes (Fig. 1, C and D), suggesting that these differences were probably acquired early during thymic ontogeny. To assess whether this difference was intrinsic to hematopoietic cells or caused by extrinsic factors, hematopoietic progenitor cells from either LEW or BN bone marrow were differentiated in the same thymic (LEW × BN) F1 environment. Although similar levels of chimerism were achieved in (LEW × BN) F1 recipients regardless of the donor origin, higher percentages of CD4$^+$ Foxp3$^+$ donor T cells were found in PBMCs, LNs, and spleen from F1 rats receiving BN bone marrow cells (Fig. 1 E). Thus, the difference in size of the T_{reg} cell compartment between LEW and BN rats is controlled by factors that are intrinsic to hematopoietic cells.

Fort1, a 117-kb locus on chromosome 9, controls the size of the natural T_{reg} cell population

We previously identified a 17-cM interval on chromosome 9 (c9) that controls the size of the CD45RC^{low}CD4$^+$ population in BN and LEW strains (Subra et al., 2001). Because Foxp3$^+$ T cells were restricted to this population (Fig. S1), we reasoned that the genetic control of the T_{reg} cell population

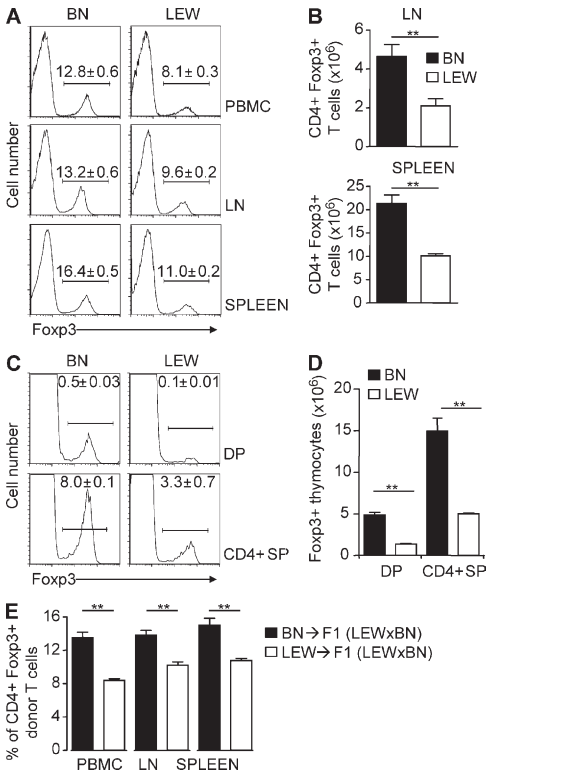

Figure 1. BN and LEW rats exhibit different proportions and numbers of natural Foxp3$^+$ T_{reg} cells. (A) Representative flow cytometry profiles of Foxp3$^+$ T cells in CD4$^+$-gated lymphocytes in PBMCs, LNs, and spleen from LEW and BN rats. The values on each cytometry profile represent the mean percentages of Foxp3$^+$ cells in the CD4$^+$ T cell population (mean ± SEM; $n = 4$). Data are representative of four independent experiments. (B) Absolute numbers (mean ± SEM) of Foxp3$^+$CD4$^+$ cells in the LNs and spleen from BN ($n = 6$) and LEW ($n = 10$) rats. (C) Representative flow cytometry profiles of Foxp3 expression in DP CD4$^+$CD8$^+$ and SP CD4$^+$CD8$^-$ thymocytes from naive BN and LEW rats. The value on each profile represents the percentages of Foxp3$^+$ thymocytes (mean ± SEM; $n = 6$). (D) Absolute numbers of Foxp3$^+$ cells in DP CD4$^+$CD8$^+$ and SP CD4$^+$ thymocytes from BN ($n = 6$) and LEW ($n = 6$) rats. Bars represent the means ± SEM. Data are representative of three independent experiments. (E) Percentages of Foxp3$^+$ cells among CD4$^+$ T cells of donor origin in PBMCs, LNs, and spleen originating from (LEW × BN) F1 recipients of bone marrow from BN or LEW rats 14 wk after engraftment. Bars represent the mean ± SEM ($n = 6$ rats per group). Data are representative of two independent experiments. **, $P < 0.01$.

might also be located in this interval. Using a panel of BN congenic lines and sublines for various LEW genomic regions of c9 (BN.LEWc9), we identified an interval of 117 kb that exerts a major effect on the proportion of CD4$^+$Foxp3$^+$ T cells (Fig. 2, A and B). Indeed, although the size of the T_{reg} cell population was unchanged in BN.LEWc9-C, -H, and -Be congenic lines when compared with BN rats, it was markedly reduced in BN.LEWc9-Ia, -B, -Bc, and -Bf congenic lines, reaching values close to those found in LEW rats. Results were similar when CD4$^+$Foxp3$^+$ T cells were analyzed in the LN, spleen, or thymus (unpublished data). In contrast, this locus, named *Fort1* for Foxp3$^+$ T_{reg} cell locus 1, did not influence the size of the conventional CD4$^+$Foxp3$^-$ compartment (Fig. S2). We then tested whether *Fort1* had an impact on the suppressive function of the Foxp3$^+$CD4$^+$ T cells using an in vitro assay. Purified CD4$^+$CD25$^+$ T cells from BN and Bf rats did not proliferate when cultured with allogeneic T cell–depleted APCs, indicating that they are anergic (Fig. 2 C). Importantly, they suppressed the proliferation of naive CD4$^+$ T cells from (LEW × BN) F1 rats with similar efficacy, thus showing that the in vitro suppressive potential of T_{reg} cells is independent of the genomic origin of *Fort1* (Fig. 2 D). Moreover, by using LEW.BNc9 and DA.BNc9 congenics (LEW or Dark Agouti [DA] congenic rats for BN *Fort1*) and BN-1L rats (BN rats congenic for LEW MHC), we further demonstrated that the control of *Fort1* on the size of the T_{reg} cell compartment was independent of the genetic background and MHC haplotype (Fig. S3). Thus, the 117-kb *Fort1* region contains a gene, or a set of genes, that exerts a pivotal control on the size of the T_{reg} cell compartment.

Vav1 R63W polymorphism is associated with the difference in the size of the T_{reg} cell compartment

Physical and high-density marker genetic maps of the 117-kb *Fort1* region were constructed using Celera and NCBI Rat Genome databases. We identified four genes within *Fort1*: *C3* (*Complement 3 precursor*), *Gpr108* (*G protein–coupled receptor 108*), *Trip10/Cip4* (*Cdc42-interacting protein 4*), and *Vav1* (Fig. 2 B). Because we did not find any differences in messenger RNA (mRNA) expression of these four genes between LEW, BN, and BN.LEWc9-Bf CD4 T cells (Fig. S4), we investigated differences in single nucleotide polymorphisms (SNPs) by sequencing their coding regions. The 15 SNPs identified were then genotyped in the smallest congenic line (Bf) and in four additional rat strains (DA, Piebald Virol Glaxo [PVG], Biobreeding [BB], and August Copenhagen Irish [ACI]). No polymorphism was found in the *Trip10* gene, and the polymorphisms found in *Gpr108* were synonymous, thus rendering improbable the involvement of these genes (Table I). Conversely, identification of two nonsynonymous SNPs in *C3* and *Vav1* made them strong candidates for the control of T_{reg} cell development. *Vav1* appeared to be the strongest candidate gene because it is specifically expressed in hematopoietic cells (Katzav et al., 1989), and *Fort1* control is intrinsic to hematopoietic cells (Fig. 1 E), whereas *C3* is mainly produced is the liver (Alper et al., 1969). A further argument for

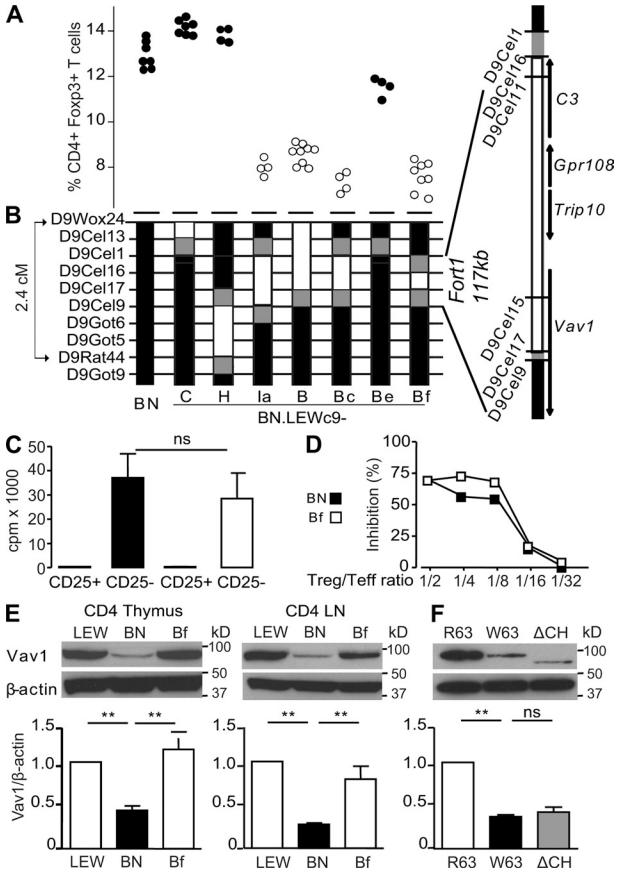

Figure 2. *Fort1*, a 117-kb locus of chromosome 9, controls the proportion of CD4$^+$Foxp3$^+$ T_{reg} cell and Vav1 protein expression. (A) Percentages of Foxp3$^+$ cells among blood CD4$^+$ T cells from the BN parental strain and a series of BN.LEWc9 congenic lines and sublines. Each point represents the value found in individual rats (n = 4–9). (B) Genetic maps of congenic lines. Microsatellite markers are indicated on the left. Black, white, and gray segments indicate chromosomal regions of BN, LEW, or undetermined origin, respectively. On the right is shown the physical map of the *Fort1* 117-kb region constructed using information from the Celera Genomics genome assembly available in the NCBI Rat Genome Resource, which contains four genes, *C3*, *Gpr108*, *Trip10*, and *Vav1*. (C) BN (closed) or Bf (open) CD25$^+$ and CD25$^-$ FACS sorted T cells were cultured for 3 d with allogeneic APCs. Proliferation was assessed with an 18-h [^{3}H]thymidine pulse added after 48 h of culture. Data represent mean ± SEM. (D) Suppressor activity of CD4$^+$CD25$^+$ T_{reg} cells was measured by T cell proliferation assay. T_{reg} cells from BN or Bf were co-cultured with effector T cells (CD4$^+$CD45RC^{high} from F1 rats) at various ratios of T_{reg} cell/T_{eff} cell. The proliferation level of responder cells alone was assigned a value of 100%. Results are representative of two independent experiments. (E) Western blot analysis of Vav1 protein expression in thymic and LN CD4$^+$ T cell lysates from LEW, BN, and Bf rats. (F) Western blot analysis of VAV1 protein in HEK293 cells transfected with plasmids encoding human wild-type VAV1 (VAV1-R63), mutated VAV1 (VAV1-W63), or oncogenic VAV1 (VAV1-ΔCH). (E and F) β-Actin was used as a loading control. In each case, results show one blot of a representative experiment and a graph representing the mean ± SEM of three to six independent experiments. **, $P < 0.01$; ns, not significant.

Table I. Vav1 variants control the percentage of CD4+Foxp3+ T_{reg} cells

Gene	Exon/nucleotide	Protein	Genotypes						
			BN	LEW	Bf[b]	DA	PVG	BB	ACI
C3	Ex2/c.205 C>T	p.=	**T**	C	C	C	C	**T**	C
C3	Ex9/c.1018 T>C	p.=	**C**	T	T	T	**C**	**C**	**C**
C3	Ex11/c.1252 C>T	p.=	**T**	C	C	C	C	**T**	C
C3	Ex12/c.1339 T>C	p.=	**C**	T	T	T	**C**	**C**	**C**
C3	Ex12/c.1369 T>C	p.=	**C**	T	T	T	**C**	**C**	**C**
C3	Ex23/c.2929 G>A	p.=	**A**	G	G	G	G	**A**	G
C3	Ex32/c.4109 A>G	p.Thr1356Ala	**G**	A	A	A	A	**G**	A
Gpr108	Ex6/c.536 G>A	p.=	**A**	G	G	G	G	**A**	G
Gpr108	Ex8/c.930 T>C	p.=	**C**	T	T	T	T	**C**	T
Gpr108	Ex8/c.935 C>T	p.=	**T**	C	C	C	C	**T**	C
Gpr108	Ex13/c.1397 G>A	p.=	**A**	G	G	G	G	**A**	G
Gpr108	Ex15/c.1520 G>A	p.=	**A**	G	G	G	G	**A**	G
Trip10	NP	NP	**NP**	NP	NP	NP	NP	**NP**	NP
Vav1[a]	Ex1/c.244 C>T[a]	p.Arg63Trp[a]	**T**	C	C	C	C	C	C
Vav1	Ex5/c.579 C>T	p.=	**C**	T	T	T	**C**	T	T
Vav1	Ex6/c.627 G>A	p.=	**A**	G	G	G	**A**	G	G

NP, no polymorphism. Genes listed are found in the 117-kb interval. The Exon/nucleotide column indicates SNPs found in exons. The exon number and the position of the SNP in the cDNA of the gene are given. The Protein column indicates the effect of the SNP (p.= indicates a synonymous mutation without effect on the primary structure of the protein; when the SNP is nonsynonymous, the position and the amino acid substitution according to the nucleotide mutation are given). Genotypes of BN type or similar to BN genotype are in bold. Mean percentages ± SEM of CD4+Foxp3+ T cells in PBMCs ($n \geq 4$) are as follows: BN, 17.0 ± 0.2%; LEW, 8.9 ± 0.9%; Bf, 11.1 ± 0.5%; DA, 10.3 ± 0.3%; PVG, 7.6 ± 0.2%; BB, 11.0 ± 0.2%; and ACI, 9.9 ± 0.5%.

[a]This mutation in the first exon of *Vav1* is the only mutation associated with the high (BN genotype) or low (other strains genotypes) percentage of CD4+Foxp3+ T cells.

[b]BN.LEWc9-Bf congenic line.

excluding the involvement of the *C3* nonsynonymous polymorphism is based on the haplotypic mapping conducted in six rat strains and in the BN.LEWc9-Bf congenic because the percentage of Foxp3+CD4+ T cells found in the BB rats is similar to that found in all the tested strains except the BN strain (Table I). Thus, the c.244C>T SNP in exon 1 of *Vav1* is the only SNP that correlates with the T_{reg} cell phenotype. This SNP results in the substitution of an arginine (R) by a tryptophan (W) in BN Vav1 at position 63 in the N-terminal calponin homology (CH) domain (p.Arg63Trp or R63W). Altogether, these results strongly suggest that the Vav1 R63W polymorphism plays a prominent role in the control of Foxp3+CD4+ T cells, in the absence of involvement of the three other genes present in the 117-kb interval.

The Vav1 R63W polymorphism controls Vav1 cellular protein levels

We next analyzed the impact of the Vav1 R63W polymorphism on Vav1 protein expression. We used rat CD4+ T cells expressing the Vav1-W63 (BN rats) or the Vav1-R63 (LEW and BN.LEWc9-Bf rats) variants. Immunoblotting revealed that levels of Vav1 were markedly lower in thymic and peripheral BN CD4+ T cells (Fig. 2 E). The same difference was also observed in CD4+CD25+ (T_{reg} cells) and in CD4+CD25− (T_{conv} cells; Fig. S5). To test whether the reduced Vav1 protein expression is the direct consequence of the R63W polymorphism, we performed experiments in HEK293 cells transfected with plasmids coding for human VAV1-R63 (wild type), VAV1-W63 (mutated), or the oncogenic human VAV1 (VAV1-ΔCH) that lacks the first 67 N-terminal amino acids and is known to be constitutively active. The protein levels of VAV1 were lower in HEK293 cells transfected with VAV1-W63 when compared with that of HEK293 cells transfected with VAV1-R63 (Fig. 2 F). A similar observation was made in HEK293 cells transfected with plasmids coding for rat Vav1 variants (unpublished data). The decreased VAV1 protein expression is also found in HEK293 cells transfected with VAV1-ΔCH (Fig. 2 F). Thus, these data show that the Vav1 R63W polymorphism impacts the cellular content of Vav1 and suggest that the Vav1-W63 variant might share biochemical and functional properties with the constitutively active VAV1-ΔCH.

Vav1 R63W polymorphism influences Vav1 functions

Vav1 functions as a guanine exchange factor (GEF) for small GTPases, thereby facilitating their transition from an inactive (GDP bound) to an active (GTP bound) state. Vav1 is also an adaptor molecule that participates in protein–protein interactions. After TCR engagement, Vav1 is rapidly phosphorylated, in particular in tyrosine 174 (Tyr174), which is crucial to Vav1 activities (Aghazadeh et al., 2000; López-Lago et al., 2000). To analyze the impact of Vav1 R63W polymorphism on Vav1 functions, we first performed biochemical experiments in HEK293 cells transfected with plasmids coding for human VAV1-R63 (wild type), VAV1-W63 (mutated), or the constitutively active VAV1 (VAV1-ΔCH). Both VAV1-W63 and

VAV1-ΔCH show increased phosphorylation on total tyrosines (Fig. 3 A) and Tyr174 (Fig. 3 B) and displayed enhanced GEF activity (Fig. 3 C) as compared with VAV1-R63. This increased GEF activity resulted in elevated activation of Rac1 (Fig. 3 D), the VAV1 preferential downstream effectors, and also in a stronger activation of RhoA (~17-fold compared with ~3-fold for Rac1; Fig. 3 E). Confocal examination of transiently transfected HEK293 cells showed that VAV1-R63 did not induce major morphological changes, whereas the expression of VAV1-W63 induced lamellipodia formation and pronounced rounding of the cell body as a result of actin cytoskeleton contractility (Fig. 3 F). These morphological changes are reminiscent of what was observed for VAV1-ΔCH

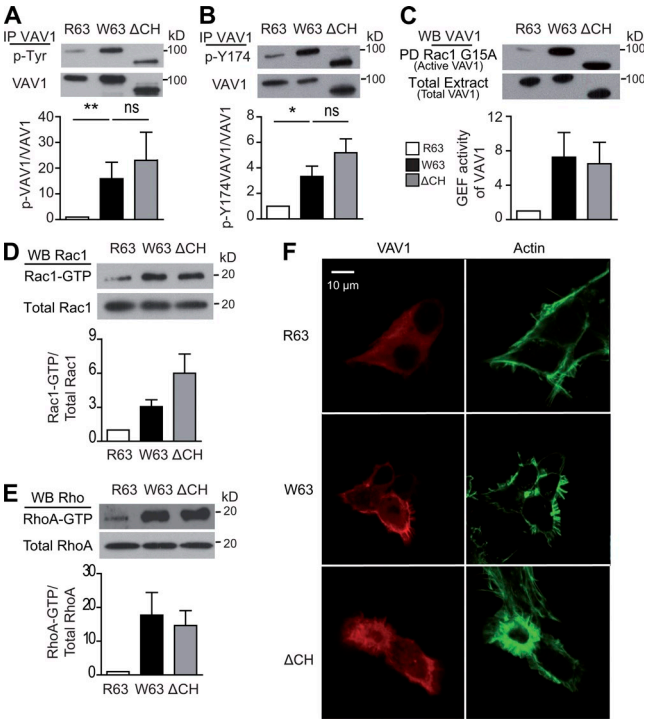

Figure 3. Biochemical analyses of VAV1 in HEK293 cells transfected with VAV1 variants reveal that VAV1-W63 is constitutively active. (A and B) Analysis of VAV1 phosphorylation in HEK293 transfected with different human VAV1 plasmids. VAV1 was immunoprecipitated and immunoblotted with anti-phosphotyrosine 4G10 mAb (A) or anti–phospho-VAV1 (Y174) antibody (B). After stripping, membranes were probed with anti-VAV1 antibody. IP, immunoprecipitation. (C) Analysis of GEF activity of VAV1 using pull-down with Rac1G15A agarose beads on serum-starved HEK293 cells transfected with different human VAV1 plasmids. (D and E) Analysis of Rac1 or RhoA activities in HEK293 cells transfected with different VAV1 variants using pull-down assay to detect relative amounts of Rac1-GTP (D) or RhoA-GTP (E). Total Rac1 and RhoA levels were used as loading controls. In each case, results show one blot of a representative experiment and a graph representing the mean ± SEM of three to four independent experiments. WB, Western blot. (F) Confocal analysis of HEK293 cells transfected with different VAV1 variants. Actin was visualized with phalloidin–Alexa Fluor 488. Representative images of three independent experiments are shown. *, $P < 0.05$; **, $P < 0.01$; ns, not significant.

(Fig. 3 F; López-Lago et al., 2000). Together, these data demonstrate that the VAV1-W63 mutation leads to its constitutive activation.

To analyze the impact of TCR engagement on Vav1 activities, we also performed biochemical analysis on purified $CD4^+$ T cells from BN (Vav1-W63) and BN.LEWc9-Bf (Vav1-R63) rats. In agreement with our results on HEK293 cells, we showed that Vav1 in BN $CD4^+$ T exhibits an increased global phosphorylation on Vav1 tyrosines (Fig. 4 A) and Tyr174 (Fig. 4 B) as compared with Bf $CD4^+$ T cells, both at basal state and after TCR engagement. However, the activation of Rac1 (Fig. 4 C) and RhoA (Fig. 4 D) GTPases was modest as compared with transfected HEK293 cells expressing similar levels of Vav1 protein. These data suggest that the increased Vav1-W63 activity in the $CD4^+$ T cells might be counterbalanced by the decrease in Vav1 protein amount, thus maintaining GEF activity close to physiological levels. Using confocal microscopy, we next showed that localization and recruitment of Vav1-W63 to TCR-inducible complexes are not altered because we observed similar colocalization of Vav1 in BN and Bf $CD4^+$ T cells (Fig. 4 E). Recently, it has been shown that many critical events involved in T cell activation, such as TCR-triggered Ca^{2+} flux, were mediated by a GEF-independent function of Vav1 that can act as an adaptor (Miletic et al., 2009; Saveliev et al., 2009). We therefore assessed the effect of R63W polymorphism on Ca^{2+} flux in thymic and peripheral $CD4^+$ T cells. $CD4^+$ T cells bearing Vav1-W63 (BN rats) had lower TCR-induced Ca^{2+} flux than those bearing Vav1-R63 (Bf and LEW rats; Fig. 4 F). Together, these data show that the Vav1 R63W polymorphism has major consequences on Vav1 biochemical properties, triggering a state of constitutive activation that leads to the imbalance between Vav1 GEF-dependent (Rac1 and RhoA activation) and -independent (Ca^{2+} flux) functions.

A recent study described the process of cooperative autoinhibition maintaining Vav1 protein in an inactive state and shed light on the molecular mechanisms whereby the Vav1-W63 variant might modify Vav1 functions (Yu et al., 2010). This work showed that the CH domain plays a key role in strengthening the interaction of the catalytic Dbl homology domain with a helix of the adjacent acidic domain, which leads to the autoinhibition of the GEF activity. This core inhibitory interaction is relieved by phosphorylation of Tyr174. The phosphorylation of two other tyrosines, Tyr142 and Tyr160, modulates the CH-inhibitory helix by making Tyr174 more accessible to kinases. Of peculiar interest, the side chain of Tyr160 is in contact with Arg63 in the CH domain (Yu et al., 2010). Based on these data, we hypothesize that replacement of the basic arginine by the hydrophobic tryptophan in position 63 might induce a modification of the tertiary structure that could make Tyr174 more accessible to phosphorylation. This mechanism would fully account for the similar behavior of the Vav1-W63 and Vav1-ΔCH variants. The activation of Vav1-W63 is associated with an approximately fourfold reduction of protein expression that

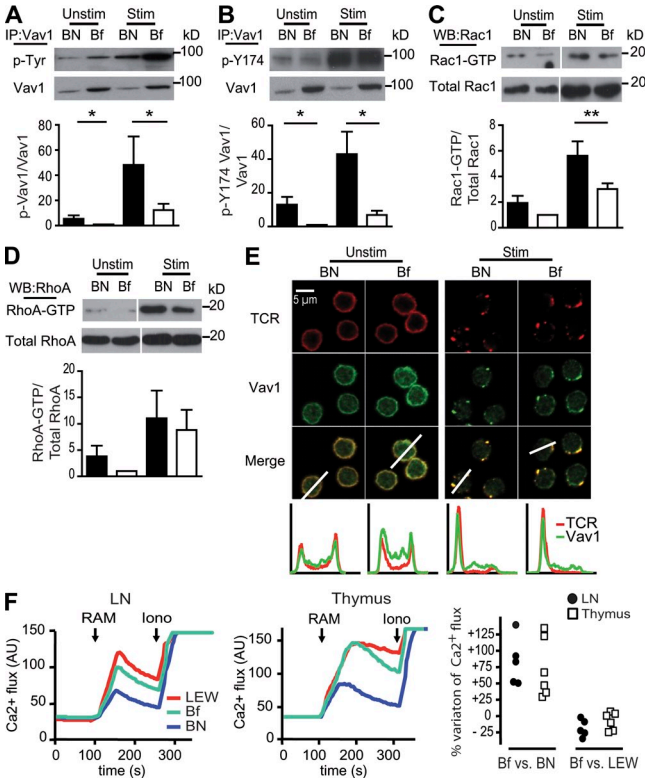

Figure 4. In primary CD4 T cells, Vav1 R63W polymorphism affects Vav1 phosphorylation, Rac1/RhoA GTPases activities, and Ca^{2+} flux under TCR stimulation. (A and B) Analysis of Vav1 phosphorylation by immunoblot with anti-phosphotyrosine 4G10 mAb (A) or anti–phospho-Vav1(Y174) antibody (B) in BN (Vav1-W63) and Bf (Vav1-R63) LN $CD4^+$ T cells stimulated (stim) or not (unstim) with anti-TCR mAb. Lysates were probed with anti-Vav1Ab. IP, immunoprecipitation. (C and D) Analysis of Rac1 or RhoA activation in serum-starved BN and Bf $CD4^+$ T cells stimulated or not with anti-TCR mAb using pull-down assay to detect the relative amounts of Rac1-GTP (C) or RhoA-GTP (D). Total Rac1 and RhoA levels were used as loading controls. In each case, results show one blot of a representative experiment and a graph representing the mean ± SEM of three to five independent experiments. WB, Western blot. (E) Confocal microscopy analyses of $CD4^+$ T cells of BN and Bf rats that were stimulated or not with anti-TCR mAb. Cells were staining for TCR (red) and Vav1 (green) using the appropriate second reagents. Line scan analysis indicates the distribution of the TCR and Vav1 along the white lines. Representative images of three independent experiments are shown. (F) Analysis of Ca^{2+} influx in purified $CD4^+$ T cells from LEW, BN, and Bf LNs (left) or thymus (middle) loaded with Indo-1 and incubated with an anti-TCR mAb. Analyses were first performed in the absence of rabbit anti–mouse (RAM) immunoglobulin cross-linker to measure the baseline Ca^{2+} level in unstimulated $CD4^+$ T cells. Flow was halted for the addition of 50 µg/ml RAM (first arrow). The increase in intracellular Ca^{2+} flux was then recorded in real time over 200 s. Cell flow was again halted for the addition of ionomycin (Iono; second arrow) to measure the maximal signal from the Indo-1 indicator. Data are representative of three independent experiments involving a total of five or six rats per strain. These data are expressed in the right panel as percentages of the variation of maximum Ca^{2+} flux observed in the Bf congenic subline compared with the BN (left) and LEW (right) parental strains.

might maintain Vav1 GEF activity close to normal levels but would impact Vav1 GEF-independent functions as revealed by the reduction of Ca^{2+} flux. Together with a recent study showing that Vav1 GEF activity is not required for the development of $CD4^+CD25^+$ T cells (Saveliev et al., 2009), these observations suggest that Vav1-W63 could influence T_{reg} cell development through an effect on Vav1 GEF-independent functions.

The link between the Vav1-W63 variant and the development of the T_{reg} cells remains unknown. The size of the T_{reg} cell compartment can be altered through modulations of the strength of TCR signals. For example, enrichment in T_{reg} cells was observed when TCR signaling was enhanced by the loss of the tyrosine phosphatase SHP-1, a negative regulator of TCR-mediated signaling (Carter et al., 2005). Enrichment was also observed when developing T cells were exposed to their cognate peptides with high-avidity interactions (Jordan et al., 2001; van Santen et al., 2004; Cabarrocas et al., 2006). Thus, in rats carrying the Vav1-W63 variant, the increased development of T_{reg} cells might result from Vav1-W63–dependent modifications in signaling pathways downstream of the TCR.

Given the link existing between T_{reg} cell defects and autoimmunity (Sakaguchi et al., 2008), our findings may have important implications. We recently provided evidence that Vav1 R63W variants play a central role in susceptibility to experimental autoimmune encephalomyelitis and impact the production of IFN-γ and TNF (Jagodic et al., 2009; unpublished data). Our present findings suggest that this may also be related to the effect of Vav1 variants on the T_{reg} cell compartment. Thus, genetic or acquired alterations in Vav1-dependent signaling could impact the susceptibility to immune-mediated diseases through effects on T_{reg} cell development.

MATERIALS AND METHODS

Animals. All breeding and experimental procedures were performed in accordance with European Union guidelines and were approved by the national and local ethics committee (license no. 31259; agreement no. B315558). Rats were kept under specific pathogen-free conditions. LEW, BN, and DA rats were obtained from Centre d'Élevage Janvier (Le Genest St. Isle, France). (LEW × BN) F1 rats and congenic lines were produced in our animal facility. The BN congenic lines for LEW chromosome 9 (BN.LEWc9) used in this study are summarized in Table S1 and were developed in our laboratory as described previously (Mas et al., 2004). The LEW.BNc9 and DA.BNc9 congenic lines for BN chromosome 9 and the BN congenic for LEW MHC (BN-1L) were described previously (Cautain et al., 2001; Jagodic et al., 2009). The animals used in this study were 8–12 wk of age.

Antibodies, cell staining, and flow cytometry. The mAbs used for flow cytometry or purification of T cell subpopulations were as follows: W3/25 (anti–rat CD4), OX6 (anti–rat MHC class II), OX8 (anti–rat CD8), OX12 (anti–rat κ light chain), OX22 (anti–rat CD45RC), OX39 (anti–rat CD25), R73 (anti–rat TCR-αβ), V65 (anti–rat TCR-γδ), 3.4.1 (anti–rat CD8αβ), and 3.2.3 (anti–rat NKR-P1). The hybridomas OX6, OX7, OX8, OX12, OX22, OX39, OX40, OX85, and W3/25 were provided by D. Mason (University of Oxford, Oxford, England, UK), and the hybridomas JJ319, V65, and R73 were provided by T. Hünig (University of Würzburg, Würzburg, Germany). The mAbs used for flow cytometry were fluorochrome conjugates either prepared in our laboratory or purchased from BD and eBioscience. The biotinylated mAbs 42-3-7 ($RT1-A^n$ haplotype) and 163-7F3 ($RT1-A^l$ haplotype) were

provided by H. Kunz (University of Pittsburgh, Pittsburgh, PA). Foxp3 intracellular expression was detected using an APC-labeled anti–mouse/rat Foxp3 Staining Set from eBioscience according to their standard protocol. Data were collected on FACSCalibur or LSRII cytometers (BD) and analyzed using FlowJo or Cell Quest software package (BD).

Bone marrow chimeras. (LEW × BN) F1 rats were lethally irradiated (950 rads) 1 d before bone marrow transplantation. Recipient rats were given 10^8 viable nucleated bone marrow cells intravenously. 14 wk after engraftment, the PBMCs, spleen, and LNs were analyzed for T cells of donor or recipient origin by using RT1-A haplotype–specific mAbs and for expression of Foxp3 in $CD4^+$ T cells of donor origin.

Purification of T cell subsets. Rat $CD4^+$ T cells were negatively selected from LN and spleen cells by using a cocktail of the following mAbs: OX6, OX8, OX12, 3.2.3, and V65. After washing and incubating with anti–mouse IgG magnetic microbeads (Invitrogen), $CD4^+$ T cells were purified by magnetic depletion. Both OX8 and W3/25 were added to the cocktails for the purification of a non–T cell fraction that included B cells and monocytes/macrophages. SP $CD4^+$ thymocytes T cells were negatively selected from thymus using OX8 mAb and anti–mouse IgG magnetic microbeads. The purity of $CD4^+$ T cells was >92%. For T_{reg} cell purification, negatively selected $CD4^+$ T cells were stained with 341-FITC (anti–rat CD8β), R73-APC (anti–rat TCR-αβ), W3/25-PB (anti–rat CD4), and OX39-PE (anti–rat CD25) and were electronically sorted using a FACSAria II-Sorp (BD). The purity of the cells was >99%.

Proliferative responses and T_{reg} cell suppression assays. For T_{reg} cell suppression assays, purified (LEW × BN) F1 $CD4^+CD45RC^{high}$ T cells (10^5/well) were stimulated with irradiated allogeneic APCs (0.5×10^5/well; T cell–depleted splenocytes from DA rats) alone or in the presence of decreased numbers of FACS-sorted BN or Bf $CD4^+CD25^+$ T_{reg} cells and cultured in 96-well plates for 72 h. Proliferation was analyzed by [^{3}H]thymidine incorporation during the last 18 h.

Sequencing. The sequencing templates were amplified from genomic DNA, and the sequencing reactions were performed using the BigDye terminator version 3.1 (Applied Biosystems) Products were separated and recorded on an ABI 3100 (Applied Biosystems). Sequences were analyzed with Vector NTI software (InforMax). SNPs identified by comparing LEW and BN coding sequences and untranslated regions of all genes in the region of 117 kb were subsequently typed in additional rat strains using the same procedures.

Plasmids, DNA constructs, mutagenesis, and transfection. Experiments were performed using human VAV1 to benefit from the availability of a positive control, the oncogenic human VAV1 (VAV1-ΔCH) that lacks the first 67 N-terminal amino acids (VAV1-ΔCH) and is known to be constitutively active. pEF-VAV1-myc plasmid encoding either human VAV1 cDNA or oncogenic human VAV1 was described previously (Deckert et al., 1996). The mutation in human VAV1 at the position c.244C>T (R63W) of the sequence coding for the R63W substitution was introduced by site-directed mutagenesis using the QuikChange II XL Site-Directed Mutagenesis kit (Agilent Technologies) according to the manufacturer's instructions. Mutation was introduced using the following primers: forward, 5′-GAGGTCAACCTGtGGCCCCAGATGTCCC-3′; and reverse, 5′-GGGACATCTGGGGCCaCAGGTTGACCTCA-3′. The lower case letters indicate the mutations. The nucleotide sequence of each construct was verified by DNA sequencing. HEK293 fibroblasts were maintained in Dulbecco's modified Eagle's medium supplemented with 10% FCS. HEK293 cells were transfected using Effectene (QIAGEN) according to the manufacturer's instructions. Experiments were performed 20 h after transfection.

Relative quantification of mRNAs by real-time quantitative RT-PCR. Total RNA was extracted by the RNeasy mini kit (QIAGEN). RT was performed using Superscript III Reverse transcription (Invitrogen). Real-time PCR was performed on LC480 (Roche) using the PCR SYBR green kit (Roche). The relative amount of mRNA in each sample was calculated as the ratio between the target mRNA and the corresponding endogenous control GAPDH mRNA.

Ca^{2+} flux. $CD4^+$ T cells or $CD4^+$ SP thymocytes were loaded at 37°C for 30 min with the fluorescent Ca indicator Indo-1 (Invitrogen) at 5 μM. The cells were then washed and incubated with 10 μg/ml anti-TCR mAb (R73) at 37°C for 15 min. Ca influx was measured by flow cytometry on an LSRII. Baseline levels were measured for 50–100 s, at which time rabbit anti–mouse (Sigma-Aldrich) was added at 50 μg/ml as a cross-linker. Events were recorded for an additional 150–200 s. Finally, ionomycin was added at 2 μg/ml to all samples to verify Indo-1 labeling. Relative Ca concentrations were measured as the ratio between the Ca-bound dye and the Ca-free dye. Data were analyzed using FlowJo software.

Immunoblotting and immunoprecipitation. Vav1 protein expression and phosphorylation were analyzed on lysates from rat $CD4^+$ T cells or from HEK293 cells 20 h after transfection with 2 μg of human wild-type VAV1-R63, the mutated VAV1-W63, or oncogenic VAV1-ΔCH plasmids. In some experiments, rat $CD4^+$ T cells were stimulated with anti-TCR mAb (R73) used at 10 μg/ml and rabbit anti–mouse at 50 μg/ml for 1 min at 37°C. Total cellular proteins were extracted with ice-cold lysis buffer containing 10 mM Tris HCl, 1% Triton X-100, a cocktail of protease inhibitors (Complete Mini, EDTA-free; Roche), 50 mM NaF, 1 mM Na_3VO_4, and 1 mM DTT. For immunoprecipitation, clarified homogenates were incubated overnight at 4°C with the antibodies and a mix of protein A/G Sepharose beads. After washes, proteins were eluted with Laemmli buffer and analyzed by SDS-PAGE followed by Western blotting on Immobilon-P membranes (Millipore) with appropriate antibodies (Vav-1 antibody, clone D7 [Santa Cruz Biotechnology, Inc.]; β-actin antibody, clone AC-15 [Sigma-Aldrich]; phosphotyrosine antibody, clone 4G10 [Millipore]; and phosphotyrosine 174 of Vav1 antibody [Santa Cruz Biotechnology, Inc.]). Immunoreactive bands were detected by chemiluminescence with the SuperSignal detection system (Thermo Fisher Scientific). Band intensities were quantified using the Scion Image software.

GTPase pull-down assays. HEK293 cells were transfected with 1 μg of wild-type VAV1-R63 or 2 μg of mutated VAV1-W63 or 2 μg of oncogenic VAV1-ΔCH. 3 h after transfection, cells were serum-starved overnight before being processed. The amounts of GTP-bound active Rac1 or RhoA were determined by GST pull-down assay. Cells were lysed in ice-cold lysis buffer (50 mM Tris-base, pH 7.4, 500 mM NaCl, 10 mM $MgCl_2$, 2.5 mM EGTA, 1% Triton X-100, 0.5% Na deoxycholate, 0.1% SDS, 50 mM NaF, 1 mM Na_3VO_4, and a tablet of protease and phosphatase inhibitors), and clarified lysates were incubated with 30 μg GST-PBD (PAK1-binding domain for Rac1) or GST-RBD (Rhotekin-binding domain for RhoA) bound to glutathione Sepharose at 4°C for 30 min. Beads were washed with 50 mM Tris-base, pH 7.4, 150 mM NaCl, 1 mM $MgCl_2$, 5 mM EGTA, 1% Triton X-100, and GTP-bound GTPases eluted with Laemmli buffer and subjected to SDS-PAGE followed by Western blotting. Active VAV1 was purified using the nucleotide-free mutant Rac1G15A (Cell Biolabs Inc.), which displays a strong affinity for active GEFs (García-Mata et al., 2006). VAV1 was detected by Western blotting using VAV1 antibody (D7 clone; Santa Cruz Biotechnology, Inc.) on pull-down cell extracts.

Immunofluorescence staining. Freshly isolated CD4 T cells were incubated for 15 min with 10 μg/ml mouse anti–rat TCR at 4°C. CD4 T cells were then stimulated or not with 50 μg/ml goat anti–mouse IgG for 15 min. Cells were fixed with 4% paraformaldehyde and plated on 0.5 mg/ml poly-DL-ornithine (Sigma-Aldrich) for 15 min. Upon washing with PBS, cells were permeabilized with 0.1% Triton X-100, saturated with 1% BSA, and incubated with antibody against Vav1 (1:200 dilution; Santa Cruz Biotechnology, Inc.) for 20 min at room temperature. Secondary antibodies used were Alexa Fluor 594–conjugated streptavidin and Alexa Fluor 488–conjugated anti–rabbit

(Invitrogen). HEK293 transfected with different variants of VAV1 were cultured on polyornithine-coated coverslips, fixed, and permeabilized as described above. Actin was visualized with phalloidin–Alexa Fluor 488. The preparations were analyzed by confocal microscopy using an LSM710 (Carl Zeiss) equipped with a 63× objective. Images were processed with ImageJ (National Institutes of Health).

Statistical analysis. Statistical analyses were performed by using the Instat statistical package (GraphPad Software). Data are expressed as means ± SEM. The significance of differences observed between two groups was analyzed by the Mann-Whitney test. When more than two groups were investigated simultaneously, the Kruskall-Wallis test was first performed.

Online supplemental material. Fig. S1 shows that $CD4^+$ $Foxp3^+$ T cells are contained within the $CD45RC^{low}$ subset. Fig. S2 shows that *Fort1* controls T_{reg} cell numbers with no effect on the size of the T_{conv} cell compartment. Fig. S3 shows that *Fort1* controls $CD4^+Foxp3^+$ (T_{reg} cell) numbers independently of the genetic background and the MHC. Fig. S4 shows mRNA expression of the four genes within the *Fort1* 117-kb region. Fig. S5 shows Vav1 expression and phosphorylation in $CD25^-$ and $CD25^+$ CD4 T cells in BN and BN.LEWc9-Bf (Bf) rats. Table S1 shows the genetic map of BN.LEWc9 congenic lines and sublines used for *Fort1* genetic dissection. Online supplemental material is available at http://www.jem.org/cgi/content/full/jem.20102191/DC1.

We thank the staff of the different platforms of our research center (Flow Cytometry, Imaging, and Animal Housing) for excellent assistance that was instrumental for the proper realization of this work. We thank Daniel Gonzalez-Dunia and Etienne Joly for critical reading of the manuscript and insightful comments.

This work was supported by Institut National de la Santé et de la Recherche Médicale, the Arthritis Fondation Courtin, Association Française contre les Myopathies, Agence Nationale de la Recherche (ANR-08-GENO-041-01), Association de Recherche sur la Sclérose en Plaques, Fondation pour la Recherche Médicale, Association de la Recherche contre le Cancer, and Région Midi-Pyrénées and Fight-MG (FP7-Health-2009-242210). A. Casemayou is supported by a grant from Fondation pour la Recherche Médicale. T. Olsson and M. Jagodic received grant support from Neuropromise (LSH-CT-2005-018637), EURATools (LSHG-CT-2005-0190115), the Swedish Research Council, and the Söderberg Foundation.

The authors have no conflicting financial interests.

Author contributions: C. Colacios and A.S. Dejean designed the research, generated bone marrow chimeras, performed flow cytometry experiments, and analyzed the data. A. Casemayou and F. Gaits-Iacovoni designed and conducted the biochemistry and cell signaling experiments. I. Bernard conducted the purification of T cell subsets. C. Pedros performed the suppression assays. D. Lagrange, M. Jagodic, and G. Fournié generated and characterized the congenic rats. L. Lamouroux and M. Jagodic performed the sequencing, mutagenesis, and PCR. M. Deckert provided human Vav1 plasmids. R. Liblau and T. Olsson contributed to the design of experiments. G. Fournié and A. Saoudi coordinated the project, designed the research, and wrote the paper.

Submitted: 15 October 2010
Accepted: 24 August 2011

REFERENCES

Aghazadeh, B., W.E. Lowry, X.Y. Huang, and M.K. Rosen. 2000. Structural basis for relief of autoinhibition of the Dbl homology domain of proto-oncogene Vav by tyrosine phosphorylation. *Cell*. 102:625–633. http://dx.doi.org/10.1016/S0092-8674(00)00085-4

Alper, C.A., A.M. Johnson, A.G. Birtch, and F.D. Moore. 1969. Human C'3: evidence for the liver as the primary site of synthesis. *Science*. 163:286–288. http://dx.doi.org/10.1126/science.163.3864.286

Cabarrocas, J., C. Cassan, F. Magnusson, E. Piaggio, L. Mars, J. Derbinski, B. Kyewski, D.A. Gross, B.L. Salomon, K. Khazaie, et al. 2006. Foxp3+ CD25+ regulatory T cells specific for a neo-self-antigen develop at the double-positive thymic stage. *Proc. Natl. Acad. Sci. USA*. 103:8453–8458. http://dx.doi.org/10.1073/pnas.0603086103

Carter, J.D., G.M. Calabrese, M. Naganuma, and U. Lorenz. 2005. Deficiency of the Src homology region 2 domain-containing phosphatase 1 (SHP-1) causes enrichment of CD4+CD25+ regulatory T cells. *J. Immunol*. 174: 6627–6638.

Cautain, B., J. Damoiseaux, I. Bernard, H. van Straaten, P. van Breda Vriesman, B. Boneu, P. Druet, and A. Saoudi. 2001. Essential role of TGF-beta in the natural resistance to experimental allergic encephalomyelitis in rats. *Eur. J. Immunol*. 31:1132–1140. http://dx.doi.org/10.1002/1521-4141(200104)31:4<1132::AID-IMMU1132>3.0.CO;2-N

Deckert, M., S. Tartare-Deckert, C. Couture, T. Mustelin, and A. Altman. 1996. Functional and physical interactions of Syk family kinases with the Vav proto-oncogene product. *Immunity*. 5:591–604. http://dx.doi.org/10.1016/S1074-7613(00)80273-3

Fontenot, J.D., J.P. Rasmussen, L.M. Williams, J.L. Dooley, A.G. Farr, and A.Y. Rudensky. 2005. Regulatory T cell lineage specification by the forkhead transcription factor foxp3. *Immunity*. 22:329–341. http://dx.doi.org/10.1016/j.immuni.2005.01.016

Fournié, G.J., B. Cautain, E. Xystrakis, J. Damoiseaux, M. Mas, D. Lagrange, I. Bernard, J.-F. Subra, L. Pelletier, P. Druet, and A. Saoudi. 2001. Cellular and genetic factors involved in the difference between Brown Norway and Lewis rats to develop respectively type-2 and type-1 immune-mediated diseases. *Immunol. Rev*. 184:145–160. http://dx.doi.org/10.1034/j.1600-065x.2001.1840114.x

García-Mata, R., K. Wennerberg, W.T. Arthur, N.K. Noren, S.M. Ellerbroek, and K. Burridge. 2006. Analysis of activated GAPs and GEFs in cell lysates. *Methods Enzymol*. 406:425–437. http://dx.doi.org/10.1016/S0076-6879(06)06031-9

Gupta, S., S. Manicassamy, C. Vasu, A. Kumar, W. Shang, and Z. Sun. 2008. Differential requirement of PKC-theta in the development and function of natural regulatory T cells. *Mol. Immunol*. 46:213–224. http://dx.doi.org/10.1016/j.molimm.2008.08.275

Hsieh, C.S., Y. Liang, A.J. Tyznik, S.G. Self, D. Liggitt, and A.Y. Rudensky. 2004. Recognition of the peripheral self by naturally arising CD25+ CD4+ T cell receptors. *Immunity*. 21:267–277. http://dx.doi.org/10.1016/j.immuni.2004.07.009

Jagodic, M., C. Colacios, R. Nohra, A.S. Dejean, A.D. Beyeen, M. Khademi, A. Casemayou, L. Lamouroux, C. Duthoit, O. Papapietro, et al. 2009. A role for VAV1 in experimental autoimmune encephalomyelitis and multiple sclerosis. *Sci. Transl. Med*. 1:10ra21. http://dx.doi.org/10.1126/scitranslmed.3000278

Jordan, M.S., A. Boesteanu, A.J. Reed, A.L. Petrone, A.E. Holenbeck, M.A. Lerman, A. Naji, and A.J. Caton. 2001. Thymic selection of CD4+CD25+ regulatory T cells induced by an agonist self-peptide. *Nat. Immunol*. 2:301–306. http://dx.doi.org/10.1038/86302

Josefowicz, S.Z., and A. Rudensky. 2009. Control of regulatory T cell lineage commitment and maintenance. *Immunity*. 30:616–625. http://dx.doi.org/10.1016/j.immuni.2009.04.009

Katzav, S., D. Martin-Zanca, and M. Barbacid. 1989. vav, a novel human oncogene derived from a locus ubiquitously expressed in hematopoietic cells. *EMBO J*. 8:2283–2290.

Koonpaew, S., S. Shen, L. Flowers, and W. Zhang. 2006. LAT-mediated signaling in $CD4^+CD25^+$ regulatory T cell development. *J. Exp. Med*. 203:119–129. http://dx.doi.org/10.1084/jem.20050903

López-Lago, M., H. Lee, C. Cruz, N. Movilla, and X.R. Bustelo. 2000. Tyrosine phosphorylation mediates both activation and downmodulation of the biological activity of Vav. *Mol. Cell. Biol*. 20:1678–1691. http://dx.doi.org/10.1128/MCB.20.5.1678-1691.2000

Mas, M., P. Cavaillès, C. Colacios, J.F. Subra, D. Lagrange, M. Calise, M.O. Christen, P. Druet, L. Pelletier, D. Gauguier, and G.J. Fournié. 2004. Studies of congenic lines in the Brown Norway rat model of Th2-mediated immunopathological disorders show that the aurothiopropanol sulfonate-induced immunological disorder (Aiid3) locus on chromosome 9 plays a major role compared to Aiid2 on chromosome 10. *J. Immunol*. 172:6354–6361.

Medoff, B.D., B.P. Sandall, A. Landry, K. Nagahama, A. Mizoguchi, A.D. Luster, and R.J. Xavier. 2009. Differential requirement for CARMA1 in agonist-selected T-cell development. *Eur. J. Immunol*. 39:78–84. http://dx.doi.org/10.1002/eji.200838734

Miletic, A.V., D.B. Graham, K. Sakata-Sogawa, M. Hiroshima, M.J. Hamann, S. Cemerski, T. Kloeppel, D.D. Billadeau, O. Kanagawa,

M. Tokunaga, and W. Swat. 2009. Vav links the T cell antigen receptor to the actin cytoskeleton and T cell activation independently of intrinsic Guanine nucleotide exchange activity. *PLoS ONE.* 4:e6599. http://dx.doi.org/10.1371/journal.pone.0006599

Ouyang, W., O. Beckett, Q. Ma, J.H. Paik, R.A. DePinho, and M.O. Li. 2010. Foxo proteins cooperatively control the differentiation of Foxp3+ regulatory T cells. *Nat. Immunol.* 11:618–627. http://dx.doi.org/10.1038/ni.1884

Sakaguchi, S., T. Yamaguchi, T. Nomura, and M. Ono. 2008. Regulatory T cells and immune tolerance. *Cell.* 133:775–787. http://dx.doi.org/10.1016/j.cell.2008.05.009

Saveliev, A., L. Vanes, O. Ksionda, J. Rapley, S.J. Smerdon, K. Rittinger, and V.L. Tybulewicz. 2009. Function of the nucleotide exchange activity of vav1 in T cell development and activation. *Sci. Signal.* 2:ra83. http://dx.doi.org/10.1126/scisignal.2000420

Subra, J.F., B. Cautain, E. Xystrakis, M. Mas, D. Lagrange, H. van der Heijden, M.J. van de Gaar, P. Druet, G.J. Fournié, A. Saoudi, and J. Damoiseaux. 2001. The balance between CD45RChigh and CD45RClow CD4 T cells in rats is intrinsic to bone marrow-derived cells and is genetically controlled. *J. Immunol.* 166:2944–2952.

Turner, M., and D.D. Billadeau. 2002. VAV proteins as signal integrators for multi-subunit immune-recognition receptors. *Nat. Rev. Immunol.* 2:476–486. http://dx.doi.org/10.1038/nri840

Tybulewicz, V.L. 2005. Vav-family proteins in T-cell signalling. *Curr. Opin. Immunol.* 17:267–274. http://dx.doi.org/10.1016/j.coi.2005.04.003

van Santen, H.M., C. Benoist, and D. Mathis. 2004. Number of T reg cells that differentiate does not increase upon encounter of agonist ligand on thymic epithelial cells. *J. Exp. Med.* 200:1221–1230. http://dx.doi.org/10.1084/jem.20041022

Wan, Y.Y., H. Chi, M. Xie, M.D. Schneider, and R.A. Flavell. 2006. The kinase TAK1 integrates antigen and cytokine receptor signaling for T cell development, survival and function. *Nat. Immunol.* 7:851–858. http://dx.doi.org/10.1038/ni1355

Yu, B., I.R. Martins, P. Li, G.K. Amarasinghe, J. Umetani, M.E. Fernandez-Zapico, D.D. Billadeau, M. Machius, D.R. Tomchick, and M.K. Rosen. 2010. Structural and energetic mechanisms of cooperative autoinhibition and activation of Vav1. *Cell.* 140:246–256. http://dx.doi.org/10.1016/j.cell.2009.12.033

Zheng, Y., and A.Y. Rudensky. 2007. Foxp3 in control of the regulatory T cell lineage. *Nat. Immunol.* 8:457–462. http://dx.doi.org/10.1038/ni1455